

1 **Positive Selection on Rare Variants Underlying the Cold Adaptation of**  
2 **Wild Boar**

3 Jianhai Chen<sup>1,2,3</sup>, Ivan Jakovlić<sup>4</sup>, Mikhail Sablin<sup>5</sup>, Shengqian Xia<sup>2</sup>, Zhixiang Xu<sup>1</sup>, Yapin Guo<sup>1</sup>,  
4 Renzuo Kuang<sup>1</sup>, Jie Zhong<sup>6</sup>, Yangying Jia<sup>2</sup>, Thuy Nhien Tran Thi<sup>7</sup>, Hao Yang<sup>8</sup>, Hong Ma<sup>9</sup>,  
5 Nikica Šprem<sup>10</sup>, Jianlin Han<sup>11</sup>, Di Liu<sup>9</sup>, Yunxia Zhao<sup>1,11,\*</sup>, Shuhong Zhao<sup>1,11,\*</sup>

6 <sup>1</sup>Key Laboratory of Agricultural Animal Genetics, Breeding and Reproduction, Ministry of Education, College of Animal  
7 Science and Veterinary Medicine, Huazhong Agricultural University, Wuhan 430070, China

8 <sup>2</sup>Department of Ecology and Evolution, The University of Chicago, 1101E 57th Street, Chicago, IL 60637, United States

9 <sup>3</sup>Institutes for Systems Genetics, Frontiers Science Center for Disease-related Molecular Network, West China Hospital,  
10 Sichuan University, Chengdu 610041, Sichuan, China

11 <sup>4</sup>State Key Laboratory of Grassland Agro-Ecosystems, and College of Ecology, Lanzhou University, 730000, Lanzhou,  
12 China. Bio-Transduction Lab, Wuhan, China

13 <sup>5</sup>Zoological Institute Russian Academy of Science, Universitetskaya nab. 1, Saint Petersburg 199034, Russia

14 <sup>6</sup>Institute of Rare Diseases, West China Hospital of Sichuan University, Sichuan University, Chengdu, 610000, China

15 <sup>7</sup>National Institute of Animal Sciences, Hanoi, Vietnam. Key Lab of Agricultural Animal Genetics, Breeding and  
16 Reproduction, Ministry of Education, College of Animal Science and Technology, Huazhong Agricultural University,  
17 Wuhan 430070, China

18 <sup>8</sup>West China-Washington Mitochondria and Metabolism Research Center; Key Lab of Transplant Engineering and  
19 Immunology, MOH, Regenerative Medicine Research Center, West China Hospital, Sichuan University, No. 88,  
20 Keyuan South Road, Hi-tech Zone, Chengdu, 610041, China

21 <sup>9</sup>Heilongjiang Academy of Agricultural Sciences, Haerbin, China

22 <sup>10</sup>Department of Fisheries, Apiculture, Wildlife Management and Special Zoology, Faculty of Agriculture, University of  
23 Zagreb, Zagreb, Croatia

24 <sup>11</sup>Yazhouwan National Laboratory, Sanya City, Hainan Province, 572024, China

25 \*Corresponding authors: Yunxia Zhao: yxzhao@mail.hzau.edu.cn; Shuhong Zhao: shzhao@mail.hzau.edu.cn

## Abstract

The wide geographical distribution of Eurasian wild boar (*Sus scrofa*) offers a natural experiment to study the thermoregulation. Here, we conducted whole-genome resequencing and chromatin profiling experiments on the local populations from cold regions (northern and northeastern Asia) and warm regions (southeastern Asia and southern China). Using genome-wide scans of four methods, we detected candidate genes underlying cold-adaptation with significant enrichment of pathways related to thermogenesis, fat cell development, and adipose tissue regulation. We also found two enhancer variants under positive selection, an intronic variant of *IGF1R* (rs341219502) and an exonic variant of *BRD4* (rs327139795), which showed the highest differentiation between cold and warm region populations of wild boar and domestic pigs. Moreover, these rare variants were absent in outgroup species and warm-region wild boar but nearly fixed in cold-region populations, suggesting their *de novo* origins in cold-region populations. The experiments of CUT&Tag chromatin profiling showed that rs341219502 of *IGF1R* is associated with the gain of three novel transcription factors involving regulatory changes in enhancer function, while rs327139795 of *BRD4* could result in the loss of a phosphorylation site due to amino acid alteration. We also found three genes (*SLCO1C1*, *PDE3A*, and *TTC28*) with selection signals in both wild boar and native human populations from Siberia, which suggests convergent molecular adaptation in mammals. Our study shows the adaptive evolution of genomic molecules underlying the remarkable environmental flexibility of wild boar.

**Key words:** selective sweep, allele frequency, cold adaptation, enhancer, CUT&Tag

## 49    **Introduction**

50    One of the most fundamental questions in evolution is to understand how populations  
51    could adapt new environment (1, 2). The peripheral or marginal population, which  
52    inhabits the boundary of a species' distribution area, is a valuable model for us to  
53    understand this question. Peripheral populations often migrate from their ancestral  
54    territories to adapt to new niches through population expansion. These populations  
55    face harsher and sometimes insurmountable environmental conditions at boundary  
56    zones, such as extreme low temperatures and a scarcity of food resources, which  
57    impede their further territorial expansion. The adaptation in challenging survival  
58    conditions make them ideal natural experiments for investigating the genetic bases of  
59    novel adaptive strategies in the face of environmental constraints.

60    Advancements in sequencing technology and population genetics are increasingly  
61    enabling the identification of functional genetic variants under natural selection for  
62    organisms to adapt new environments (3-8). Strong selective forces in derived  
63    populations would leave distinguished genomic signals segregating from source  
64    populations (2, 9). To discern selective signals in peripheral populations, studies often  
65    explore the patterns of multiple genomic parameters, including allele frequencies (2,  
66    10-12), nucleotide diversity (13-15), and haplotype segregation (16, 17). For example,  
67    human populations have adapted to diverse environments, ranging from the tropical  
68    African regions to the cold peripheral regions of Siberia. Genome-wide scan based on  
69    patterns of haplotype and allele frequency in Siberian populations reveals selective  
70    signals of genes underlying cold adaptation (3). By exploring variants of these  
71    candidate genes, a globally low-frequency nonsynonymous variant in *CPT1A* has been  
72    identified as the most likely causative mutation, due to its high allele frequency in local  
73    Siberian populations (18).

74    In this study, we focus on the wild boar, *Sus scrofa*, a species with remarkable adaptive  
75    capabilities and wide distribution across diverse climatic regions in Eurasia. Their

ecological niches encompass the humid tropics of Southeast Asia, extend through temperate zones, and reach the extreme area of the Qinghai-Tibet plateau as well as subarctic Siberia (19, 20). Phylogenetic analyses suggest that the Eurasian wild boar diverged from a clade of closely related *Sus* species at the onset of the Pliocene epoch (5.3-3.5 million years ago) within the tropical Asia (21). Subsequently, between 1 and 2 million years ago, the species expanded beyond tropical Asia across a substantial range of Eurasia, establishing various geographically distinct populations (19). Biogeographic studies have revealed a migratory trajectory of the wild boar from southern to northern Asia (22, 23). This long-range migration of wild boar suggests that populations from tropical and Siberian regions are source and peripheral populations, respectively. Thus, wild boar could serve as a natural animal model to investigate genetic bases subject to positive selection in response to novel climatic challenges under cold environment.

Following their migration from tropical Asia, wild boar have established their northernmost natural habitat in Siberia, reaching as far as 61°N (20). Given the species' tropical origins, we hypothesize that the genomes of cold-region populations could exhibit signals of adaptation to colder climates. However, this hypothesis has not yet been empirically tested (20). Here, we conducted the whole-genome sequencing of wild boar populations from both tropical Asian and Siberian regions. We identified candidate genes and related biological pathways underlying cold adaptation of wild boar. Based on these selective genes, we detected the leading variants with the highest cold-warm differentiation and site-level signal of selective sweep among all regulatory and missense variants. We further explored functional implications of the leading variants with experiments of the Cleavage Under Targets and Tagmentation (CUT&Tag). Our study provides insights into the positively selected genes and rare variants potentially underlying the bioclimatic adaption of cold-region wild boar.

## Results

### The phylogenetic origin of wild boar from cold and warm regions

We obtained a total of 821 Gb whole-genome data from 11 new samples: six wild boar from Siberia and five from Southeast Asia (Figure 1a). After mapping to the pig genome reference (Sscrofa v11.1), the average sequencing depth was estimated to be 28.32x. We compiled two datasets for different analytical purposes, featuring varied sample sizes: a core dataset comprising 63 genomes, and an extended dataset encompassing 488 genomes (Supplementary Tables 1 and 2). Using a distance matrix based on identity by state (IBS) and the neighbor-joining method, we initially evaluated the phylogenetic relationships for all 488 samples (Figure 1b). We revealed that eastern Siberian samples (E, F, and G in Figure 1a) clustered within the clade of wild boar populations from northern China, northeastern China, and northeastern Asia (South Korea and Japan) (D), while the western Siberian samples (H in Figure 1a) clustered with the European wild boar. The southeastern Asian wild boar clustered close to the wild boar and indigenous breeds from southern China.

For the core dataset, we conducted the principal component analysis (PCA) and IBS phylogenetic inference to validate population relationships (Figure 1c). These analyses revealed similar population phylogeny with the relationship obtained with the extended dataset (Figure 1b). Specifically, our newly sequenced tropical population (B) clustered together with the temperate wild boar from southern China (C in Figure 1). The newly sequenced Siberian population was divided into two clusters (E, F, and G vs. H, Figure 1c), consistent with the pattern produced by the extended dataset (Figure 1b). These results revealed higher divergence between the populations from western (H) and eastern Siberia (E, F, and G), but close relationship between tropical (B, Vietnam) and temperate Asian wild boar populations (southern China, C). These results also

indicated a substantial genomic differentiation between peripheral populations of cold regions and source populations in tropical regions.

Gene flow between the western and eastern Siberian populations was examined utilizing TreeMix (v1.12) (24) (Supplementary Figure 1b-d). This analysis identified the optimal number of migration events ( $m$ ) as three, which explained over 99.8% of the variance in genetic relatedness among the populations (Supplementary Figure 1b-c). Notably, the inferred migration events suggested a predominant westward gene flow from eastern to western Siberian populations (Supplementary Figure 1d). Further analysis on population structure was conducted using ADMIXTURE v1.3 (25), with a cross-validation approach pinpointing the optimal number of distinct ancestries at  $K=4$  (Supplementary Figure 1a). An investigation into the ancestral composition, considering ancestry counts from two to four, distinguished two primary clades correlating with the established ancestries of Eurasian wild boar and domestic pigs, namely Asian and European lineages (Figure 1d). This division was corroborated by Principal Component Analysis (PCA) and phylogenetic assessments, elucidating the major population relationships (Figures 1b and 1c). Intriguingly, the population in western Siberia exhibited a 9.64% composition of Asian ancestry when analyzed at  $K=3$  (Figure 1d), suggesting a restricted gene flow from Asia towards the western Siberian demographic.

### **The genes under selective sweep and their functional enrichment in thermogenic and adipose-related pathways**

Extensive research has suggested that 1% - 15% of genes in the mammalian genome may undergo positive Darwinian selection (26-28). For instance, in humans, approximately 10% of genes are believed to be under positive selection, though the concordance rates among different statistical tests typically range from 8% to 27% (27, 28). In our study, employing four complementary analytical approaches (Materials and

Methods), we identified candidate genes showing evidence of selective pressure in cold-region wild boar, including those native to Siberia, northern and northeastern China, and northeastern Asia (Supplementary Table 2-7). Our comprehensive analysis revealed that 1.54% of genes (313 out of 20,306, Ensembl v105) were consistently identified across at least three distinct methods as being under selection, indicating a conservative estimation in this study. Additionally, 0.45% of genes (92 out of 20,306) were corroborated by all four analytical methods (Supplementary Table 7).

We analyzed the functional enrichment for genes supported by at least three methods (Figure 2a, Supplementary Table 8). We revealed four pathways potentially related to cold resistance: the 'thermogenesis' pathway (*ADCY9*, *NDUFB6*, *PPARG*, *PRKACB*, *SMARCC1*, *TSC2*), the 'regulation of cold-induced thermogenesis' pathway (*ACADL*, *IGF1R*, *JAK2*, *NOVA1*, *NOVA2*), the 'positive regulation of adipose tissue development' pathway (*PPARG*, *NCOA2*, *SIRT1*), and the 'fat cell differentiation' pathway (*PPARG*, *TGFB1*, *SIRT1*, *WWTR1*) ( $p < 0.05$ , Figure 2a). These findings indicate that specific pathways—especially those governing thermogenesis and fat cell differentiation—may play a critical role in enabling cold-region wild boars to adapt to their harsh environmental conditions.

By analyzing genetic variants whose allele frequencies were higher in wild boar from cold region (Siberia, Korea, northern and northeastern China) than in those from warmer regions (temperate and tropical Asia), we uncovered a long haplotype block with strong linkage disequilibrium (LD,  $\Delta dAF_{cold-warm} > 0.5$ ,  $D' > 0.9$ ) among variants of seven genes (*FAM169B*, *PGPEP1L*, *IGF1R*, *SYNM*, *TTC23*, *LRRC28*, and *MEF2A*). Surprisingly, this region is the longest gene cluster we identified with selective signals, spanned 1.3 Mb on chromosome 1 (137.2 Mb-138.5 Mb, Figure 2b). Among these linked genes, *IGF1R*, known as the Insulin-like Growth Factor 1 Receptor, received support from all four methods (Supplementary Table 7), suggesting the reliability of positive selection on this gene. Using the HKA-like test (29), we identified *IGF1R* as

the most distinguished gene with the highest reduction of polymorphism relative to divergence, supporting a significant deviation from neutral evolution (Figure 2c). At population level, *IGF1R*, *ALDH1A2*, and *PGPEP1L* showed the highest inter-population divergences between cold and warm region wild boar among all protein-coding genes ( $F_{st} = 0.65$ , Figure 2d and Supplementary Table 3). Notably, among these three genes, *IGF1R* demonstrated the highest reduction in nucleotide diversity for cold region wild boar compared to warm region ones (Figure 2d), suggesting a strong positive selection on linked variants beneficial to cold adaptation. These results of natural selection on *IGF1R* are consistent with the extensive *in vivo* studies on mice, which have revealed the role of *IGF1R* in thermoregulation, particularly in reducing core body temperature in response to cold stress and calorie restriction (30, 31).

### **The potential convergent evolution for Siberian mammals.**

The endothermic mammalian species inhabiting cold regions like Siberia may have shared genes under convergent selection for cold resistance. To test this hypothesis, we retrieved genes under positive selection for cold adaptation in Siberian human populations, which were inferred with iHS and XP-EHH methods (top 1% windows) in a previous study (3) (Supplementary Table 9). We focused on shared genes with rigorous support from four methods (Supplementary Table 7), and found three consensus genes, *SLCO1C1*, *PDE3A*, and *TTC28*, which could be under convergent evolution. We confirmed the signals of positive selection for these genes based on nucleotide diversity comparison between cold- and warm-region populations and the HKA test (Supplementary Figure 2).

### **The most differentiated intronic and exonic variants were detected in *IGF1R* and *BRD4*, respectively.**

Natural selection, driven by emerging selective forces, can result in the increased frequency or fixation of derived alleles, as well as the decreased frequency or loss of



ancestral alleles within a peripheral population due to novel adaptation (18, 32). The causative variants within genes under positive selection are expected to show pronounced allele frequency divergence between peripheral and source populations (18). This principle has also been applied extensively in medical genetics to find disease variants (33-35). By analyzing polymorphic variants across 92 candidate genes identified by all four approaches of selection screening (Supplementary Table 7), we identified the variant exhibiting the greatest allele frequency difference ( $\Delta dAF_{\text{cold-warm}}$ ) between cold- and warm-region wild boar populations for both regulatory and exonic variants.

For regulatory variants, we identified the highest  $\Delta dAF_{\text{cold-warm}}$  in an intronic variant of *IGF1R* (NC\_010443.5:g.137677482C>T, c.94+12830G>A, intron 1, rs341219502), demonstrating the highest differentiation of allele frequency ( $\Delta dAF_{\text{cold-warm}} = 0.896$ ). We validated the selection on this variant with the method of extended haplotype homozygosity (EHH) (32, 36). We observed a decay of haplotype homozygosity with increasing distance from the focal core allele (Figure 3a). The EHH decays were far more rapid for the ancestral variant haplotypes (blue curve) than for derived variant haplotypes (red curve, Figure 3b). This signal of positive selection was also supported by the inter-population changes of nucleotide diversity ( $\pi$ ) and the level of polymorphism relative to divergence (Supplementary Figure 3a). The nucleotide diversity ( $\pi$ ) in the vicinity of rs341219502 was significantly lower in cold-region wild boar populations compared to their warm-region counterparts (the chi-square test,  $p < 1.2 \times 10^{-4}$ ). Consistently, a significant deficiency of derived polymorphic variants surrounding rs341219502 in cold-region wild boar was found compared to polarized divergent sites at the interspecific level (chi-square test,  $p < 2.2 \times 10^{-16}$ ). Allele frequency distribution indicated that this variant was absent in tropical Asian populations but was fixed (100%) in northern Asian wild boar populations (Figure 3c). The cross-species orthologous alignment of Amniota vertebrates (Ensembl v105)

revealed that the ancestral state 'C' is very conserved in *Suidae* species, from *Catagonus wagneri* to 13 pig breeds, indicating that the 'C' allele is highly conserved and likely represents the ancestral state (Supplementary Figure 3b). All these findings supported the recent selective sweep in the region surrounding rs341219502 of *IGF1R*.

For exonic variants, we annotated variants with disruptive or protein-altering effects. Based on  $\Delta dAF_{\text{cold-warm}}$ , we revealed a missense derived variant of *BRD4* (NC\_010444.4:g.62317232G>A, c.1043G>A, p.Ser348Asn, rs327139795) with the highest cold-warm differentiation ( $\Delta dAF_{\text{cold-warm}} = 0.854$ ), among all exonic variants. We observed the decreased nucleotide diversity in the cold-region populations relative to the warm-region populations and the reduced polymorphism relative to the divergence in cold-region populations (Supplementary Figure 3c). We also found the delayed decay of derived haplotype homozygosity (Figure 3d-3e). These findings support the hypothesis of recent positive selection acting on this variant. The nucleotide mutation from 'G' to 'A' resulted in an amino acid change from Ser to Asn in the second exon of *BRD4*. The multiple species alignment revealed that the ancestral state of the variant 'G' is very conserved among mammals (Supplementary Figure 3d). We did not observe the derived allele 'A' in nine outgroup species, including African warthogs, pygmy hogs, and *Sus* species, which suggests that the derived allele 'A' should have originated after the speciation of *Sus scrofa*. We did not detect the derived 'A' allele in wild boar populations from Southeast Asia or Europe, suggesting its East Asian origin (Figure 3f). Among the East Asian wild populations, the derived allele of rs327139795 was nearly fixed in cold-region populations (96.30%) but was a rare allele in warm-region populations (2.78%). The homozygotes of derived allele "AA" were widespread in cold-region samples (92.59%, 25/27) but absent in warm-region populations (0%, 0/18).

**The potential *de novo* origin and recent selective sweep of rs341219502 and rs327139795 in cold-region wild boar**

Three candidate scenarios could account for the evolutionary origin of the derived alleles rs341219502 and rs327139795: (1) In the first scenario, the two alleles appeared *de novo* in the cold-region population; (2) In the second scenario, the low-frequency standing variant was transferred from warm-region populations to cold-region populations via gene flow; and (3) In the third scenario, the two alleles appeared *de novo* in the domestic pigs (within last 10,000 years), and then were transferred to cold-region populations via gene flow.

To distinguish between the first two scenarios, we applied gene flow analysis on the genomic region around the focal variants. The localized TreeMix analysis on the genomic regions upstream and downstream of the intronic variant rs341219502 in *IGF1R* (137.3 Mb - 137.6 Mb) indicated gene flow from cold-region populations towards warm-region populations (EANW to EASW in Supplementary Figure 4a). Phylogenetic relationships confirmed this direction of gene flow (Supplementary Figure 4b-c). Specifically, in the background topology of chromosome 1, East Asian wild boar populations were divided into the warm clade and cold clade (Supplementary Figure 4b). However, the local haplotype tree around rs341219502 revealed that five warm-clade haplotypes dispersed into the cold-clade (Supplementary Figure 4c), suggesting the replacement of some warm-clade haplotypes by those from the cold-clade, a typical gene flow process. Thus, the presence of the derived 'T' allele in two warm-region wild boar samples likely resulted from southward gene flow from cold-region population. For the exonic variant rs327139795, due to the small number of genic variants (only 21), we expanded our analysis to include broader surrounding regions of the focal variant (61.5 - 63 Mb) and estimated the local gene flow events with TreeMix. The result supported the direction of gene flow from cold- to warm-region wild boar (Supplementary Figure 4d). This observation further suggests that the low frequency of allele 'A' in rs327139795 in the warm-region population was most likely introduced into the warm-region population via gene flow from cold regions.

To assess the possibility of the third scenario, we examined the allele frequency distribution among 353 domestic pigs (Supplementary Table 10). We did not detect the derived 'T' allele of rs341219502 in either European or southern Chinese domestic pig populations, while being rare variants in East Asian northern and western domestic pigs with low frequencies (2.98% and 4.81%, respectively). Only 2.55% (9/353) of northern Chinese domestic samples carried this derived allele in Min, Meishan, and Tibetan breeds. Moreover, a majority of domestic genotypes (8/9) carrying the derived allele were heterozygous, while only a single Tibetan domestic pig was homozygous. In sharp contrast to this distribution, 93.3% (28/30) genotypes of this allele in cold-region wild populations from Japan, Korea, Siberia, and northern China were homozygous. As for rs327139795, allele 'A' homozygotes in European and Chinese domestic populations were also rare (1.07% and 6.58%, respectively). Notably, among all domestic pigs, individuals homozygous for the variant were rare, comprising only 0.28% (1/353) of the population for rs341219502.

Therefore, it is less likely that these two derived alleles originated from domestic pigs. The patterns observed in the origin and rise of rs341219502 and rs327139795 are consistent with the most parsimonious interpretation of a *de novo* origin in wild boar. The alternative hypothesis that these variants originate from ancestral polymorphism is also less plausible because no such variants have been found in Southeast Asian and European wild boars, nor in outgroup species within the Suidae family. Given that the divergence time between Northern and Southern Chinese wild boars falls within 25,000 to 50,000 years ago (37, 38), the age of these two variants could be under 50,000 years. Subsequent to their *de novo* emergence, natural selection likely facilitated their fixation across wild populations in cold regions.

**The transcriptional changes in rs341219502 of *IGF1R* and post-translational changes in rs327139795 of *BRD4*.**

Fat and diencephalon are among the tissues responsible for an animal's ability to withstand cold temperatures (39, 40). Thus, we investigated the expression of *IGF1R* in fat and diencephalon tissues of the Min pig, which is a local breed in cold region of northeastern China. We collected tissue samples from individuals carrying the mutant allele of *IGF1R*. The RNA-seq expression analysis showed that *IGF1R* has high levels of expression in fat and diencephalon of the adult Min pig (Figure 4a). Based on public data of H3K4me1 ChIP-seq for adipose and cerebellum, we revealed that the rs341219502 resides within the enhancer region of the first intron of *IGF1R* (Supplementary Figure 5), suggesting the importance of this variant on regulating gene expression.

Subsequently, we performed the CUT&Tag experiment (41) and found the H3K27ac modification around *IGF1R* (Figure 4b). Specifically, the signals corresponding to the rs341219502 variant were observed within the enhancer region of the first intron of *IGF1R* (Figure 4c). This result confirms the role of this variant on regulating gene expression. The prediction of transcription factor (TF) motif showed that the derived allele 'T' could gain three novel TF binding sites, including the NFATC3, SPI1 and RFX5 (Figure 4d). Thus, we analyzed the expression of these three TFs with RNA-seq and found their stable expression in adipose and diencephalon tissues (Figure 4e). These findings indicate that the rs341219502 derived allele 'T' is an enhancer mutation, which could potentially enhance the activity of the *IGF1R* enhancer by introducing novel binding sites for these transcription factors.

We also performed analysis on *BRD4*, a gene also expressed in both adipose tissues and the diencephalon. The H3K27ac modification enrichment were detected around the *BRD4* and its exonic variant rs327139795 (Figure 4f-h). Contrastingly, transcription factor (TF) motif analyses did not identify any TF binding sites at the locus of the *BRD4* exonic variant rs327139795 (Fig. 4i). As this variant resides on the exon of *BRD4*, we further analyzed the amino acid type of allele G and A (rs327139795). The results

showed when the genomic sequence changes from G to A, the amino acid at this location (348aa) changes from Serine to Asparagine (Figure 4j). Serine, typically a phosphorylation site, upon substitution to Asparagine, is predicted to result in the loss of this phosphorylation capability. To substantiate this prediction, phosphorylation site analysis of both wild-type *BRD4* and the rs327139795 variant was performed using the NetPhos 3.1 software, which leverages neural network ensembles. The analysis confirmed the loss of the phosphorylation site at the amino acid position 348 upon substitution of Serine with Asparagine (Fig. 5k).

### **The demographic history does not support the ‘genetic drift’ hypothesis.**

Another question that remains open is: were the selected alleles near-fixed in cold-region populations via the positive Darwinian selection or genetic drift? The fact that we detected strong signals of positive selection on the two sites (rs341219502 and rs327139795) supports the first hypothesis, however, rapid genetic drift can sometimes leave patterns similar to those caused by positive selection (42), so it is necessary to further test the drift hypothesis. As a rapid genetic drift would require a strong reduction in the historical effective population size, we formally evaluated it using PopSizeABC, a simulation-based demographic history inference method operating under the framework of approximate Bayesian computation (ABC). We evaluated the ancestral dynamics of effective population size for both warm- and cold-region wild populations of Asian origin. Based on population-level diploid genomes for warm- and cold-region populations (15 and 21, respectively), 100 independent 2 Mb-long regions, and 600,000 simulated datasets of the same size, we revealed different trends of demographic changes between warm- and cold-region populations ranging from 100,000 years ago to 1,000 years ago. Multiple studies found that the divergence time between Northern and Southern Chinese wild boar is within the range of 25,000 to 50,000 years ago (37, 38), which suggests that wild boar may have arrived in northern China before this period, so this time range

367 covered the upper and lower limits of the divergence time between northern and  
368 southern Chinese wild boar. The prediction errors of PopSizeABC inference were  
369 within the acceptable range (43) (Supplementary Figure 6). We found a steadily  
370 increasing, rather than declining, trend of historical population size for the cold-region  
371 wild boar populations during the period of ~25,000 to 50,000 years ago (Figure 5). In  
372 contrast, the population sizes in warm-region wild boar populations decreased  
373 sharply during this period. Thus, the increasing trend of population size history in  
374 cold-region wild boar does not support the rapid genetic drift hypothesis.

## Discussion

A key challenge in biology is to map out the functional elements within the genome and to understand their roles in adaptive processes. Natural selection can create distinctive patterns in the genomic regions surrounding the positively selected genes, which deviate from those predicted under neutral evolution. Several key indicators—including characteristic variations in genetic diversity, shifts in allele frequencies, and divergences between species—serve as critical tools in the identification of genes under positive selection that are integral to complex adaptations (14, 16, 44-47). For example, research focusing on the plateau wild boar has uncovered genes with selective signals that are vital for coping with severe environmental conditions (47-50). Moreover, the haplotype approach has revealed a significant section of the X chromosome that is involved in climate adaptation in both wild and domestic pig populations from northern China and Europe (16). These studies have substantially deepened our understanding of the dynamics of natural selection.

Northern Asia, encompassing the vast expanse of Siberia, is characterized by its extremely cold winters, posing significant challenges to endothermic mammals in maintaining thermal balance. The severe low temperatures serve as a strong selective force, especially for species like the wild boar, necessitating adaptations for effective thermoregulation in these frigid zones. Beyond the cold, another major environmental challenge is the scarcity of food resources during the lengthy winter season (20). Thus, uncovering molecular adaptations enabling peripheral or derived populations of wild boar to survive and flourish in the cold Siberian climate and its neighboring regions is a subject of great scientific interest.

In this study, employing whole-genome sequencing and four selective sweep scan methodologies, we pinpointed candidate genes that are implicated in cold adaptation. Our pathway analysis indicated several key biological processes, notably in regulating



fat cell differentiation, fostering adipose tissue development, thermogenesis, and cold-induced thermogenesis. These insights confirm that brown adipose tissue is essential for thermogenic adaptation to cold, triggering diverse processes involving neural, vascular, and metabolic responses to cold, as revealed from studies in humans, mice, insects, and polar mammals (51-54). Three positively selected genes (*SLCO1C1*, *PDE3A*, and *TTC28*) were also reported in indigenous Siberian human populations (3). Interestingly, the association between low temperature and SNPs near *SLCO1C1* and *PDE3A* has been also found in Holstein cattle (55). Thus, it is likely that these genes are under recurrent convergent evolution in mammals due to their interactive functions for the cold resistance (4, 56).

At gene level, *IGF1R* is particularly interesting considering extensive studies on its gene functions in thermoregulation. Transgenic mice studies have revealed that *IGF1R* can reduce core body temperature under the joint effect of cold stress and calorie restriction (30, 31). *IGF1R* may also have a role in body size regulation (57-59). Among all variants, an intronic variant with most probably regulatory impact (rs341219502, c.94+12830G>A, reverse strand) in *IGF1R* and a missense variant (rs327139795, c.1043G>A, forward strand) in *BRD4* showed the strongest differentiation between the cold- and warm-region populations. Notably, *BRD4* was also among the genes supported by all four methods of selective sweep scans. These two mutations, 'T' of rs341219502 and 'A' of rs327139795, are absent from all included outgroup Suidae and Tayassuidae species. At the population scale, the alleles are fixed only in cold-region wild boar while rare or absent in warm-region wild boar that are closer to the origin place of pig species (Southeast Asia), which strongly suggests their *de novo* origin in cold-region wild population. Although the two alleles were found in a tiny fraction of the southern Chinese wild boar population and Tibetan domestic pigs, it is most probable that the allele was introduced from northern populations by gene flow, based on the evidence of local TreeMix signals (or phylogeny misplacement), very low

allele frequencies, and extremely high heterozygosity rate of allele-carrying individuals from these groups.

Moreover, our CUT&Tag experiment revealed that the derived allele of rs341219502 is located in the enhancer region of *IGF1R*. We validated the enhancer signals of this variant in both fat and diencephalon tissues of the Min pig, a local breed adapted to cold environment of northeastern China. The allele transition from 'C' to 'T' could result in novel binding targets of TFs, including NFATC3, SPI1 and RFX5, to the enhancer. Interestingly, previous studies showed that NFATC3 is required for cardiac development and mitochondrial function (60). NFATC3 can also increase insulin sensitivity, controlling gene expression influencing the development and adaptation of numerous mammalian cell types including the adipocyte and neurons (61). The SPI1 (PU.1) can inhibit adipocyte differentiation (62, 63). The RFX5 can regulate resistance to nutrient stress (64). Moreover, the 'A' allele of rs327139795 within the exon of BRD4 leads to a change from Serine to Asparagine. Based on the basic feature of amino acid, the changing from Serine to Asparagine could affect phosphorylation sites, which may cause changes in the interaction between the mutated Asparagine and surrounding amino acids, thereby potentially affecting protein function.

## Conclusions

The wild boar (*Sus scrofa*) has been remarkably successful in colonizing Eurasia, notably their rapid expansion from tropical Asia into a diverse array of climates. This includes their movement into the extreme cold of arctic Siberia less than a million years ago. Through whole-genome sequencing and employing multiple methods of summary statistics, including the allele frequency spectrum ( $F_{st}$  and the ratio of  $\theta_{\pi}$ ), haplotype, and species divergence, we identified genes under selective sweeps in cold-region populations. These genes were found to enrich metabolic pathways critical for cold

resistance, including thermogenesis, fat cell development, and the regulation of adipose tissue. The most pronounced selection signal was identified in a 1.3 Mb region on chromosome 1, characterized by linkage disequilibrium surrounding *IGF1R*. At the variant level, a regulatory variant within *IGF1R* and a missense variant within *BRD4* showed the most significant differentiation in allele frequency between the warm- and cold-region populations. Analysis of allele frequency distribution suggests a de novo origin for these variants within cold-region wild populations. The demographic reconstruction revealed that the rise of these variants was unlikely to be attributable to random effects (such as genetic drift). Considering the known functions of *BRD4* and *IGF1R* in bioenergy homeostasis and body temperature regulation (30, 65, 66), our study provides insight into the molecular adaptation to the cold climate in free-range wild boar populations from Siberia and nearby regions.

## Materials and methods

### DNA sampling, sequencing, variants calling, and datasets

The genomic DNA was extracted from hair follicles of five Vietnamese wild boar (Son La province, Vietnam, ~20°N), three wild boar from the Novosibirsk region (Novomyhaylovka village, Kochenyovskiy district, Latitude 55°17'35"N, Longitude 81°48'38"E), one wild boar from Tyva (~51°N), one wild boar from Buryat (~51°N), and one wild boar from Zabaykalsky Krai (~52°N). Whole-genome sequencing (WGS) was performed on all samples using the DNBSEQ-T7 platform (MGI) with a paired-end library (2 × 125 bp).

Whole-genome mapping and calling processes were largely conducted following a previously devised methodology (16, 67, 68). In short, whole-genome short-reads data for 26 samples representing wild boar from cold (Siberia and northern Asia, 11 samples) and warm regions (temperate and tropical Asia, 11 samples), and outgroup species (4 samples), were cleaned using fastp software with default parameters (69) and subsequently mapped to the genomic reference of Sscrofa 11.1 with BWA v0.7.17 (70). Although there are multiple reference-level assembled genomes for pigs, including multiple domestic breeds (71, 72) and the wild boar (68), we chose the Sscrofa11.1 as the reference due to its high annotation and sequencing quality (73). For the variant calling, we jointly used two software programs: SAMtools v1.15.1 (74) and GATK v4.2.6.1 (<https://gatk.broadinstitute.org/hc/en-us>). The major steps included marking duplicates, recalibrating base quality scores, per-sample calling with HaplotypeCaller, and joint-calling with GenotypeGVCFs. We filtered variants using the expression "QUAL < 100.0 || QD < 2.0 || MQ < 40.0 || FS > 200.0 || SOR > 10.0 || MQRankSum < -12.5 || ReadPosRankSum < -8.0".

Two datasets were composed for analyses of specific purposes. The simplified core dataset of 63 samples (Supplementary Table 1) was used for almost all analyses

except the initial confirmation of population identity and the allele frequency distribution analysis. For this core dataset, the analyzed samples included 24 wild boar from northern and northeastern China to represent the cold region population, 24 wild boar from southern China, Sumatra, and southern Europe (Italy and Greece) to represent the warm region populations, and 15 samples of four different *Sus* species (*Sus verrucosus*, *Sus celebensis*, *Sus cebifrons*, *Sus barbatus*) as outgroups (16, 75) (Supplementary Table 1). The other dataset was much larger: 488 samples. This dataset was used to confirm the population identity of new samples and evaluate the allele frequency distribution across geographical populations (Supplementary Table 2). This dataset incorporated new samples (11 samples) and the public database data for 477 wild boar and domestic pig samples (Supplementary Table 2). The geographic populations were divided into the European wild boar (EUW, 47 samples), East Asian northern wild boar (EANW, 30 samples), East Asian southern wild boar (EASW, 18 samples), southeastern Asian wild boar (SEAW, 8 samples), and Outgroups species (OG, including African warthog, African bush hog, African red river hog, pygmy hog, Southeast Asian *Sus* species). In addition, we also included domestic pig samples: the European domestic pigs (EUD, 186 samples), East Asian northern domestic pigs (EAND, 84 samples), East Asian southern domestic pigs (EASD, 31 samples), and East Asian western domestic pigs (EAWD, which are also Tibetan pigs, 52 samples).

### **Population relationships, ancestry, and gene flow**

For the core (63 genomes) and extended (488 genomes) datasets, to understand whether sample size would influence the population relationship, we initially evaluated and compared the phylogenetic topologies of the genomes using a distance matrix derived from identity by state (IBS) calculations. For the core dataset, we also conducted the principal component (PCA) analysis to understand inter-group relationships and population clustering. The potential gene flow between western and eastern Siberian populations was evaluated with the TreeMix analysis (24). We

estimated the optimal number of migration events ( $m$ ) using OptM inference with a sufficient model threshold of 99%(76). We further conducted ancestry estimation and admixture analyses using ADMIXTURE v1.3 (25).

## **Genome-wide scan for natural selection signals in the North Asian wild boar populations**

We conducted a genome-wide scan for signals of natural selection in North Asian wild boar populations, using four complementary methods: 1. Fixation index ( $F_{st}$ ) and nucleotide diversity ratio ( $\theta_{\pi\_warm}/\theta_{\pi\_cold}$ ); 2. The XP-CLR test and nucleotide diversity ratio ( $\theta_{\pi\_warm}/\theta_{\pi\_cold}$ ) (77); 3. Extended haplotype homozygosity (EHH)-based statistic (ihh12) (78, 79); 4. Hudson–Kreitman–Aguadé (HKA)-like test (29, 80).

The fixation index ( $F_{st}$ ) and nucleotide diversity ( $\pi$ ) are among the most classical parameters, which are based on the expectation that a recent positive selection can reduce the nucleotide diversity but increase the  $F_{st}$  between two populations with differentiated phenotypes. Thus, the selected chromosomal regions for North Asian wild boar are expected to have higher  $F_{st}$  but lower  $\pi$ . The method of ihh12, a haplotype-based scan, was developed to detect both hard and soft selective sweeps, with more power than other tools (such as iHS) to detect soft sweeps (78, 79). The HKA-like test is based on the prediction from the neutral theory that species divergence (fixed site differences) and population polymorphism should be correlated (29). Departures from the strictly neutral evolution via population-level selection would result in a faster reduction of polymorphisms than species divergence (80, 81). We used inter-species differences with numbers of fixed sites (>60 SNPs) as a measure of divergence between *S. scrofa* and other four *Sus* species (*S. verrucosus*, *S. celebensis*, *S. cebifrons*, and *S. barbatus*). The XP-CLR test, which is also a cross-population composite likelihood ratio test based on the site frequency spectrum (SFS),

is a powerful test for detecting selective events restricted to a single population (77, 82).

The results from these four methods were normalized based on ranked genes and only the genes falling outside of 99% of parameter distribution were considered as significant departures from a strict neutral expectation for each method. Subsequently, to make the identification more rigorous, we considered the genes as positively selected candidates for cold adaptation only if at least three out of four methods supported them independently (Supplementary Table 7). For the positively selected sites, we further confirmed their recent positive selection signal with the method of Extended Haplotype Homozygosity (EHH) around the focal variants (32) implemented in rehh v2 (83). The ancestral-derived relationships were determined based on polarizing sites in the outgroup *Sus* species. The local phylogeny was estimated with FastTree v2.1 (84) based on haplotype consensus sequences composed using SAMtools and BCFtools v1.15 (74).

### **Functional pathway enrichment analysis for genes supported by at least three methods and allele frequency distribution for focal variant(s)**

Due to the complex nature of climatic adaptation, hundreds of genes would be responsive and under positive selection (3, 4, 56). We thus analyzed functional enrichment to understand the overall pattern of biological pathway. Only genes supported by at least three methods were used for the enrichment analysis with the Metascape database (85). The origin of the derived allele was analyzed based on the allele frequency distribution among populations and across species. The population distribution was based on the extended dataset of 488 samples (Supplementary tables 2 and 10). The focal allele across species was defined as fixed if the homozygous allele was detected in all of the outgroup samples. Ensembl v105 was used to confirm the presence or absence of an orthologous mutation based on the whole genome

alignment between *S. scrofa* (Suidae) and a species belonging to the sister family  
Tayassuidae - *Catagonus wagneri*.

## **Historical population demography for cold-region populations**

Based on the PCA, ADMIXTURE, and phylogeny, we removed the putative European-  
origin samples. After filtering out the potential recent gene flow, we kept the closely  
related samples of Asian origin to represent the cold- and temperate -region  
populations (15 samples and 21 samples, respectively). In this way, we reduced the  
impact of current population structure fluctuations on the inference of ancestral  
dynamics of the effective population size. The computation was based on the  
instructions of the PopSizeABC pipeline (43). This method applies the framework of  
approximate Bayesian computation, it can analyze more samples than similar PSMC  
(86) and MSMC (87) tools, and it is robust to sequencing errors and complex  
population dynamics (43). Specifically, we first summarized the folded allele frequency  
spectrum and the average zygotic linkage disequilibrium. Then, we simulated 400,000  
datasets under random population size histories. These pseudo-observed datasets  
(PODs) cover the same sample size and 100 independent 2 Mb-long regions.  
Ancestral population sizes were independently estimated by the ABC for each POD.  
The estimated values were compared to their true values with the tolerance rate of  
0.001.

## **The CUT&Tag and RNA-seq data collection and processing**

The samples of Cleavage Under Targets and Tagmentation (CUT&Tag) and RNA-seq  
were collected from the 180-days Min pig (a Chinese local breed) snap-frozen in liquid  
nitrogen. All the sample collected protocols were approved by the Ethics Committee  
of Huazhong Agricultural University (2022-0031). The CUT&Tag experiment followed  
the guideline of the original CUT&Tag method for tissues (41). The H3K27ac histone  
modification antibody was used to perform the antibody enrichment of CUT&Tag of fat



and diencephalon tissues of the Min pig. The RNA-seq protocols of fat and diencephalon tissues were based on the methods of rRNA-depletion and strand-specific RNA-seq provided by Illumina (Illumina, San Diego, CA). The sequencing for CUT&Tag and RNA-seq was performed with the Illumina NovaSeq6000 (PE150) platform.

The sequencing data of CUT&Tag were cleaned with the Cutadapt to trim the adapter (88). Then the clean data were mapped with Bowtie2 to the susScr11 (Sus scrofa 11.1) reference genome (89). The peak calling was performed using MACS (90). The vertebrate motif from JASPAR2020 were used to match the enhancer sequence of focal genes (91). The RNA-seq data were processed following our previous study (92).

## **Acknowledgements**

We extend special thanks to Martin Holzenberger and Bruno Conti for their patient discussion and valuable improvements to the manuscript. We also thank Evgeniy Varisovich Kamaldinov, Valeriy Lavrentyevich Petukhov, and our reviewers for their insightful comments and discussions.

## **Funding**

J.H.C acknowledges the financial support the Fifth Batch of Technological Innovation Research Projects in Chengdu (2021-YF05-01331-SN), the Postdoctoral Research and Development Fund of West China Hospital (2020HXBH087), and the Short-Term Expert Fund of West China Hospital (139190032). Dr. M.S acknowledges the financial support by ZIN RAS (state assignment № 122031100282-2). N.Š. acknowledges the financial support by the Croatian Science Foundation, project IP 2019-04-4096 “The

role of hunting related activities in the range expansion of recently established wild ungulate populations in the Mediterranean”.

## Author Contributions

J.H.C., Y.X.Z., and S.H.Z. supervised this work. J.H.C., M.S., Z.X.X, Y.P.G, R.Z.K, J.Z., Y.Y.J., T.N.T.T., T.S., H.Y, H.M, N.S., J.L.H, D.L, S.Q.X., and I.J. designed the research. J.H.C., J.Z., Z.X.X, Y.P.G, R.Z.K, J.Z., and Y.X.Z analyzed data. J.H.C. wrote the manuscript. Y.X.Z, S.H.Z, and I.J. revised the draft.

## Competing interests

The authors declare no competing financial interests.

## Data Availability Statement

The whole-genome sequence data can be accessed through NCBI BioProject code PRJNA859556.

## References

1. S. Freeman, J. C. Herron, *Evolutionary analysis* (Pearson Prentice Hall Upper Saddle River, NJ, 2007), vol. 834.
2. Y. H. Liu *et al.*, Whole-Genome Sequencing Reveals Lactase Persistence Adaptation in European Dogs. *Mol Biol Evol* **38**, 4884-4890 (2021).
3. A. Cardona *et al.*, Genome-Wide Analysis of Cold Adaptation in Indigenous Siberian Populations. *PLOS ONE* **9**, e98076 (2014).
4. P. Librado *et al.*, Tracking the origins of Yakutian horses and the genetic basis for their fast adaptation to subarctic environments. *Proceedings of the National Academy of Sciences* **112**, E6889-E6897 (2015).
5. E. Axelsson *et al.*, The genomic signature of dog domestication reveals adaptation to a starch-rich diet. *Nature* **495**, 360-364 (2013).
6. Q. Qiu *et al.*, Yak whole-genome resequencing reveals domestication signatures and prehistoric population expansions. *Nature Communications* **6**, 10283 (2015).

- 645 7. M. B. Hufford *et al.*, Comparative population genomics of maize  
646 domestication and improvement. *Nature Genetics* **44**, 808-811 (2012).
- 647 8. J. Yu *et al.*, Genome-Wide Detection of Selection Signatures in Duroc  
648 Revealed Candidate Genes Relating to Growth and Meat Quality. *G3*  
649 *Genes|Genomes|Genetics* **10**, 3765-3773 (2020).
- 650 9. J. Chen *et al.*, Population size may shape the accumulation of functional  
651 mutations following domestication. *BMC Evolutionary Biology* **18**, 4 (2018).
- 652 10. K. M. Siewert, B. F. Voight, Detecting Long-Term Balancing Selection Using  
653 Allele Frequency Correlation. *Mol Biol Evol* **34**, 2996-3005 (2017).
- 654 11. J. Chen, X. He, I. Jakovlić, Positive selection-driven fixation of a hominin-  
655 specific amino acid mutation related to dephosphorylation in IRF9. *BMC*  
656 *Ecology and Evolution* **22**, 132 (2022).
- 657 12. L. B. Barreiro, G. Laval, H. Quach, E. Patin, L. Quintana-Murci, Natural  
658 selection has driven population differentiation in modern humans. *Nature*  
659 *genetics* **40**, 340-345 (2008).
- 660 13. J. Guo *et al.*, Comparative genome analyses reveal the unique genetic  
661 composition and selection signals underlying the phenotypic characteristics of  
662 three Chinese domestic goat breeds. *Genetics Selection Evolution* **51**, 70  
663 (2019).
- 664 14. J. Chen *et al.*, The novel compound heterozygous rare variants may impact  
665 positively selected regions of TUBGCP6, a microcephaly associated gene.  
666 *Frontiers in Ecology and Evolution* **10** (2022).
- 667 15. L. Zhang *et al.*, Rapid evolution of protein diversity by de novo origination in  
668 *Oryza*. *Nature Ecology & Evolution* **3**, 679-690 (2019).
- 669 16. H. Ai *et al.*, Adaptation and possible ancient interspecies introgression in pigs  
670 identified by whole-genome sequencing. *Nature Genetics* **47**, 217-225 (2015).
- 671 17. A. Wallberg, C. Schöning, M. T. Webster, M. Hasselmann, Two extended  
672 haplotype blocks are associated with adaptation to high altitude habitats in  
673 East African honey bees. *PLoS Genet* **13**, e1006792 (2017).
- 674 18. Florian J. Clemente *et al.*, A Selective Sweep on a Deleterious Mutation in  
675 CPT1A in Arctic Populations. *The American Journal of Human Genetics* **95**,  
676 584-589 (2014).
- 677 19. M. F. Rothschild, A. Ruvinsky, *The genetics of the pig* (CABI, 2011).
- 678 20. N. Markov *et al.*, The wild boar *Sus scrofa* in northern Eurasia: a review of  
679 range expansion history, current distribution, factors affecting the northern  
680 distributional limit, and management strategies. *Mammal Review* **n/a** (2022).
- 681 21. L. A. Frantz *et al.*, Genome sequencing reveals fine scale diversification and  
682 reticulation history during speciation in *Sus*. *Genome biology* **14**, 1 (2013).
- 683 22. J. Chen *et al.*, Selective constraints in cold-region wild boars may defuse the  
684 effects of small effective population size on molecular evolution of  
685 mitogenomes. *Ecology and Evolution* **8**, 8102-8114 (2018).
- 686 23. G.-S. Wu *et al.*, Population phylogenomic analysis of mitochondrial DNA in  
687 wild boars and domestic pigs revealed multiple domestication events in East  
688 Asia. *Genome Biology* **8**, R245 (2007).

- 689 24. J. K. Pickrell, J. K. Pritchard, Inference of Population Splits and Mixtures from  
690 Genome-Wide Allele Frequency Data. *PLOS Genetics* **8**, e1002967 (2012).
- 691 25. D. H. Alexander, J. Novembre, K. Lange, Fast model-based estimation of  
692 ancestry in unrelated individuals. *Genome research* **19**, 1655-1664 (2009).
- 693 26. S. E. Harris, J. Munshi-South, Signatures of positive selection and local  
694 adaptation to urbanization in white-footed mice (*Peromyscus leucopus*).  
695 *Molecular Ecology* **26**, 6336-6350 (2017).
- 696 27. J. L. Kelley, W. J. Swanson, Positive selection in the human genome: from  
697 genome scans to biological significance. *Annu Rev Genomics Hum Genet* **9**,  
698 143-160 (2008).
- 699 28. C. D. Bustamante *et al.*, Natural selection on protein-coding genes in the  
700 human genome. *Nature* **437**, 1153-1157 (2005).
- 701 29. N. W. VanKuren, M. Long, Gene duplicates resolving sexual conflict rapidly  
702 evolved essential gametogenesis functions. *Nature Ecology & Evolution* **2**,  
703 705-712 (2018).
- 704 30. R. Cintron-Colon *et al.*, Insulin-like growth factor 1 receptor regulates  
705 hypothermia during calorie restriction. *Proceedings of the National Academy*  
706 *of Sciences* **114**, 9731-9736 (2017).
- 707 31. M. Sanchez-Alavez *et al.*, Insulin causes hyperthermia by direct inhibition of  
708 warm-sensitive neurons. *Diabetes* **59**, 43-50 (2010).
- 709 32. P. C. Sabeti *et al.*, Detecting recent positive selection in the human genome  
710 from haplotype structure. *Nature* **419**, 832-837 (2002).
- 711 33. S. Richards *et al.*, Standards and guidelines for the interpretation of sequence  
712 variants: a joint consensus recommendation of the American College of  
713 Medical Genetics and Genomics and the Association for Molecular  
714 Pathology. *Genet Med* **17**, 405-424 (2015).
- 715 34. Y. Jia *et al.*, Novel rare mutation in a conserved site of PTPRB causes human  
716 hypoplastic left heart syndrome. *Clin Genet* **103**, 79-86 (2023).
- 717 35. S. Marwaha, J. W. Knowles, E. A. Ashley, A guide for the diagnosis of rare  
718 and undiagnosed disease: beyond the exome. *Genome Medicine* **14**, 23  
719 (2022).
- 720 36. M. Gautier, R. Vitalis, rehh: an R package to detect footprints of selection in  
721 genome-wide SNP data from haplotype structure. *Bioinformatics* **28**, 1176-  
722 1177 (2012).
- 723 37. M. Zhang, Q. Yang, H. Ai, L. Huang, Revisiting the evolutionary history of  
724 pigs via De Novo mutation rate estimation in a three-generation pedigree.  
725 *Genomics, Proteomics & Bioinformatics*  
726 <https://doi.org/10.1016/j.gpb.2022.02.001> (2022).
- 727 38. M. A. M. Groenen *et al.*, Analyses of pig genomes provide insight into porcine  
728 demography and evolution. *Nature* **491**, 393-398 (2012).
- 729 39. A. Caron, S. Lee, J. K. Elmquist, L. Gautron, Leptin and brain-adipose  
730 crosstalks. *Nat Rev Neurosci* **19**, 153-165 (2018).

- 731 40. J. M. Rondeel, W. J. de Greef, W. C. Hop, D. L. Rowland, T. J. Visser, Effect  
732 of cold exposure on the hypothalamic release of thyrotropin-releasing  
733 hormone and catecholamines. *Neuroendocrinology* **54**, 477-481 (1991).
- 734 41. H. S. Kaya-Okur *et al.*, CUT&Tag for efficient epigenomic profiling of small  
735 samples and single cells. *Nature Communications* **10**, 1930 (2019).
- 736 42. N. H. Barton, J. Mallet, Natural Selection and Random Genetic Drift as  
737 Causes of Evolution on Islands [and Discussion]. *Philosophical Transactions:  
738 Biological Sciences* **351**, 785-795 (1996).
- 739 43. S. Boitard, W. Rodríguez, F. Jay, S. Mona, F. Austerlitz, Inferring Population  
740 Size History from Large Samples of Genome-Wide Molecular Data - An  
741 Approximate Bayesian Computation Approach. *PLOS Genetics* **12**, e1005877  
742 (2016).
- 743 44. D. Charlesworth, Balancing Selection and Its Effects on Sequences in Nearby  
744 Genome Regions. *PLOS Genetics* **2**, e64 (2006).
- 745 45. M. Kimura, T. Ohta, *Theoretical Aspects of Population Genetics.(MPB-4),  
746 Volume 4* (Princeton University Press, 2020), vol. 114.
- 747 46. C. Darwin, *The Origin of Species by Means of Natural Selection, Or, The  
748 Preservation of Favoured Races in the Struggle for Life* (Books, Incorporated,  
749 Pub., 1859).
- 750 47. M. Li *et al.*, Genomic analyses identify distinct patterns of selection in  
751 domesticated pigs and Tibetan wild boars. *Nature Genetics* **45**, 1431-1438  
752 (2013).
- 753 48. M. Gan *et al.*, High Altitude Adaptability and Meat Quality in Tibetan Pigs: A  
754 Reference for Local Pork Processing and Genetic Improvement. *Animals* **9**,  
755 1080 (2019).
- 756 49. H. Ai *et al.*, Population history and genomic signatures for high-altitude  
757 adaptation in Tibetan pigs. *BMC Genomics* **15**, 834 (2014).
- 758 50. Y.-F. Ma *et al.*, Population Genomics Analysis Revealed Origin and High-  
759 altitude Adaptation of Tibetan Pigs. *Scientific Reports* **9**, 11463 (2019).
- 760 51. C. L. Coolbaugh, B. M. Damon, E. C. Bush, E. B. Welch, T. F. Towse, Cold  
761 exposure induces dynamic, heterogeneous alterations in human brown  
762 adipose tissue lipid content. *Scientific Reports* **9**, 13600 (2019).
- 763 52. J. C. Chang *et al.*, Adaptive adipose tissue stromal plasticity in response to  
764 cold stress and antibody-based metabolic therapy. *Scientific Reports* **9**, 8833  
765 (2019).
- 766 53. O. Grahl-Nielsen *et al.*, Fatty acid composition of the adipose tissue of polar  
767 bears and of their prey: ringed seals, bearded seals and harp seals. *Marine  
768 Ecology Progress Series* **265**, 275-282 (2003).
- 769 54. C. Peres Valgas da Silva, D. Hernández-Saavedra, J. D. White, K. I.  
770 Stanford, Cold and Exercise: Therapeutic Tools to Activate Brown Adipose  
771 Tissue and Combat Obesity. *Biology (Basel)* **8** (2019).
- 772 55. S. Dikmen, J. B. Cole, D. J. Null, P. J. Hansen, Genome-Wide Association  
773 Mapping for Identification of Quantitative Trait Loci for Rectal Temperature  
774 during Heat Stress in Holstein Cattle. *PLOS ONE* **8**, e69202 (2013).

- 775 56. A. V. Igoshin *et al.*, Genome-wide association study and scan for signatures  
776 of selection point to candidate genes for body temperature maintenance  
777 under the cold stress in Siberian cattle populations. *BMC Genetics* **20**, 26  
778 (2019).
- 779 57. B. C. Hoopes, M. Rimbault, D. Liebers, E. A. Ostrander, N. B. Sutter, The  
780 insulin-like growth factor 1 receptor (IGF1R) contributes to reduced size in  
781 dogs. *Mammalian Genome* **23**, 780-790 (2012).
- 782 58. Brian T. O'Neill *et al.*, Differential Role of Insulin/IGF-1 Receptor Signaling in  
783 Muscle Growth and Glucose Homeostasis. *Cell Reports* **11**, 1220-1235  
784 (2015).
- 785 59. E. Grochowska *et al.*, Association of a polymorphism in exon 3 of the IGF1R  
786 gene with growth, body size, slaughter and meat quality traits in Colored  
787 Polish Merino sheep. *Meat Science* **172**, 108314 (2021).
- 788 60. P. B. Bushdid, H. Osinska, R. R. Waclaw, J. D. Molkentin, K. E. Yutzey,  
789 NFATc3 and NFATc4 Are Required for Cardiac Development and  
790 Mitochondrial Function. *Circulation Research* **92**, 1305-1313 (2003).
- 791 61. T. T. Yang *et al.*, Role of transcription factor NFAT in glucose and insulin  
792 homeostasis. *Mol Cell Biol* **26**, 7372-7387 (2006).
- 793 62. J. Rustenhoven *et al.*, PU.1 regulates Alzheimer's disease-associated genes  
794 in primary human microglia. *Molecular Neurodegeneration* **13**, 44 (2018).
- 795 63. K. Y. Chen *et al.*, Adipocyte-Specific Ablation of PU.1 Promotes Energy  
796 Expenditure and Ameliorates Metabolic Syndrome in Aging Mice. *Front Aging*  
797 **2**, 803482 (2021).
- 798 64. Z. Hu *et al.*, The transcription factor RFX5 coordinates antigen-presenting  
799 function and resistance to nutrient stress in synovial macrophages. *Nature*  
800 *Metabolism* **4**, 759-774 (2022).
- 801 65. S. Y. Kim *et al.*, Epigenetic Reader BRD4 (Bromodomain-Containing Protein  
802 4) Governs Nucleus-Encoded Mitochondrial Transcriptome to Regulate  
803 Cardiac Function. *Circulation* **142**, 2356-2370 (2020).
- 804 66. Joeva J. Barrow *et al.*, Bromodomain Inhibitors Correct Bioenergetic  
805 Deficiency Caused by Mitochondrial Disease Complex I Mutations. *Molecular*  
806 *Cell* **64**, 163-175 (2016).
- 807 67. J. Chen *et al.*, Whole-genome sequencing identifies rare missense variants of  
808 WNT16 and ERVW-1 causing the systemic lupus erythematosus. *Genomics*  
809 **114**, 110332 (2022).
- 810 68. J. Chen *et al.*, The de novo assembly of a European wild boar genome  
811 revealed unique patterns of chromosomal structural variations and segmental  
812 duplications. *Animal Genetics* **53**, 281-292 (2022).
- 813 69. S. Chen, Y. Zhou, Y. Chen, J. Gu, fastp: an ultra-fast all-in-one FASTQ  
814 preprocessor. *Bioinformatics* **34**, i884-i890 (2018).
- 815 70. H. Li, R. Durbin, Fast and accurate short read alignment with Burrows–  
816 Wheeler transform. *Bioinformatics* **25**, 1754-1760 (2009).

817 71. M. Li *et al.*, Comprehensive variation discovery and recovery of missing  
818 sequence in the pig genome using multiple de novo assemblies. *Genome*  
819 *Research* **27**, 865-874 (2017).

820 72. L. Zhang *et al.*, Development and Genome Sequencing of a Laboratory-  
821 Inbred Miniature Pig Facilitates Study of Human Diabetic Disease. *iScience*  
822 **19**, 162-176 (2019).

823 73. A. Warr *et al.*, An improved pig reference genome sequence to enable pig  
824 genetics and genomics research. *GigaScience* **9** (2020).

825 74. H. Li *et al.*, The Sequence Alignment/Map format and SAMtools.  
826 *Bioinformatics* **25**, 2078-2079 (2009).

827 75. L. A. F. Frantz *et al.*, Evidence of long-term gene flow and selection during  
828 domestication from analyses of Eurasian wild and domestic pig genomes.  
829 *Nature Genetics* **47**, 1141-1148 (2015).

830 76. R. R. Fitak, OptM: estimating the optimal number of migration edges on  
831 population trees using Treemix. *Biology Methods and Protocols* **6** (2021).

832 77. H. Chen, N. Patterson, D. Reich, Population differentiation as a test for  
833 selective sweeps. *Genome Research* **20**, 393-402 (2010).

834 78. Z. A. Szpiech, R. D. Hernandez, selscan: An Efficient Multithreaded Program  
835 to Perform EHH-Based Scans for Positive Selection. *Molecular Biology and*  
836 *Evolution* **31**, 2824-2827 (2014).

837 79. R. Torres, Z. A. Szpiech, R. D. Hernandez, Correction: Human demographic  
838 history has amplified the effects of background selection across the genome.  
839 *PLOS Genetics* **15**, e1007898 (2019).

840 80. M. J. Ford, C. F. Aquadro, Selection on X-linked Genes During Speciation in  
841 the *Drosophila athabasca* Complex. *Genetics* **144**, 689-703 (1996).

842 81. P. K. Ingvarsson, Population subdivision and the Hudson–Kreitman–Aguade  
843 test: testing for deviations from the neutral model in organelle genomes.  
844 *Genetical Research* **83**, 31-39 (2004).

845 82. F. Racimo, Testing for Ancient Selection Using Cross-population Allele  
846 Frequency Differentiation. *Genetics* **202**, 733-750 (2015).

847 83. M. Gautier, A. Klassmann, R. Vitalis, rehh 2.0: a reimplement of the R  
848 package rehh to detect positive selection from haplotype structure. *Molecular*  
849 *Ecology Resources* **17**, 78-90 (2017).

850 84. M. N. Price, P. S. Dehal, A. P. Arkin, FastTree 2—approximately maximum-  
851 likelihood trees for large alignments. *PloS one* **5**, e9490 (2010).

852 85. Y. Zhou *et al.*, Metascape provides a biologist-oriented resource for the  
853 analysis of systems-level datasets. *Nature Communications* **10**, 1523 (2019).

854 86. H. Li, R. Durbin, Inference of human population history from individual whole-  
855 genome sequences. *Nature* **475**, 493-496 (2011).

856 87. S. Schiffels, R. Durbin, Inferring human population size and separation history  
857 from multiple genome sequences. *Nature Genetics* **46**, 919-925 (2014).

858 88. M. Martin, Cutadapt removes adapter sequences from high-throughput  
859 sequencing reads. *2011* **17**, 3 (2011).

- 860 89. B. Langmead, C. Wilks, V. Antonescu, R. Charles, Scaling read aligners to  
861 hundreds of threads on general-purpose processors. *Bioinformatics* **35**, 421-  
862 432 (2018).
- 863 90. Y. Zhang *et al.*, Model-based Analysis of ChIP-Seq (MACS). *Genome Biology*  
864 **9**, R137 (2008).
- 865 91. O. Fornes *et al.*, JASPAR 2020: update of the open-access database of  
866 transcription factor binding profiles. *Nucleic Acids Research* **48**, D87-D92  
867 (2019).
- 868 92. Y. Zhao *et al.*, A compendium and comparative epigenomics analysis of cis-  
869 regulatory elements in the pig genome. *Nat Commun* **12**, 2217 (2021).  
870



**Figure 1.** The population distribution, genomic relationships, and historical demography of wild boar populations. (a) The wild boar population distribution (map retrieved from the IUCN red list: <https://www.iucnredlist.org/species/41775/44141833>). The red and blue colors indicate samples from warm and cold regions, respectively. Triangles and stars indicate populations with newly sequenced data and publicly available data, respectively. The population locations are Sumatra (A), Vietnam (B), South China (C), Northeast China and Korea (D), Zabaykalsky Krai (E), Buryat (F), Tyva (G), Novosibirsk (H), and Italy and Greece (I). (b) The phylogenetic tree for the extended dataset of 448 samples is based on IBS distances among samples. Background shadows highlight major clades, and brackets indicate newly sequenced samples. (c) The principal component analysis (PCA) and phylogenetic tree based on autosomal SNPs. In the phylogenetic tree, all major clade divisions were supported by 1000 bootstrap replicates (100%). (d) The admixture analysis (K=2, 3, 4) for population ancestry. The green color indicates the outgroup *Sus* species (*S. verrucosus*, *S. celebensis*, *S. cebifrons*, and *S. barbatus*) from the islands of Southeast Asia. The red symbols show the Southeast and East Asian population ancestry in populations from A to G. The light blue shows the European ancestry in H and I.

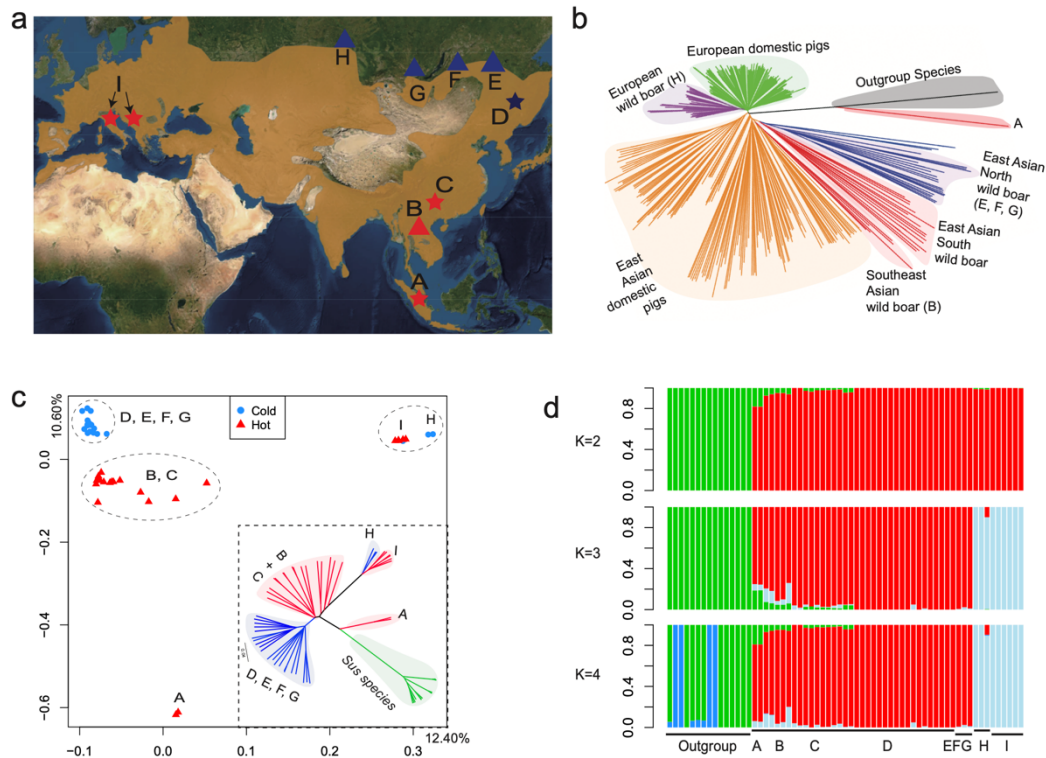


**Figure 2.** The functional enrichment and the candidate gene *IGF1R* underlying cold adaptation in the cold-region wild boar. (a) The enriched pathways were analyzed using the Metascope database (16). Only the significantly enriched pathways ( $p < 0.05$ ) are listed (Supplementary table 8). (b) Haplotype blocks for the cold and warm region samples based on variants with allele frequencies higher in cold than in warm regions ( $\Delta dAF_{cold-warm} > 0.5$ ). (c) The plot of HKA-like test. The vertical axis shows the decreased numbers of polymorphic sites relative to the counts of interspecies divergent sites. (d) The distribution of the Fixation index ( $F_{st}$ ) and nucleotide diversity ratio  $[\log_2(\theta_{\pi\_warm}/\theta_{\pi\_cold})]$ .

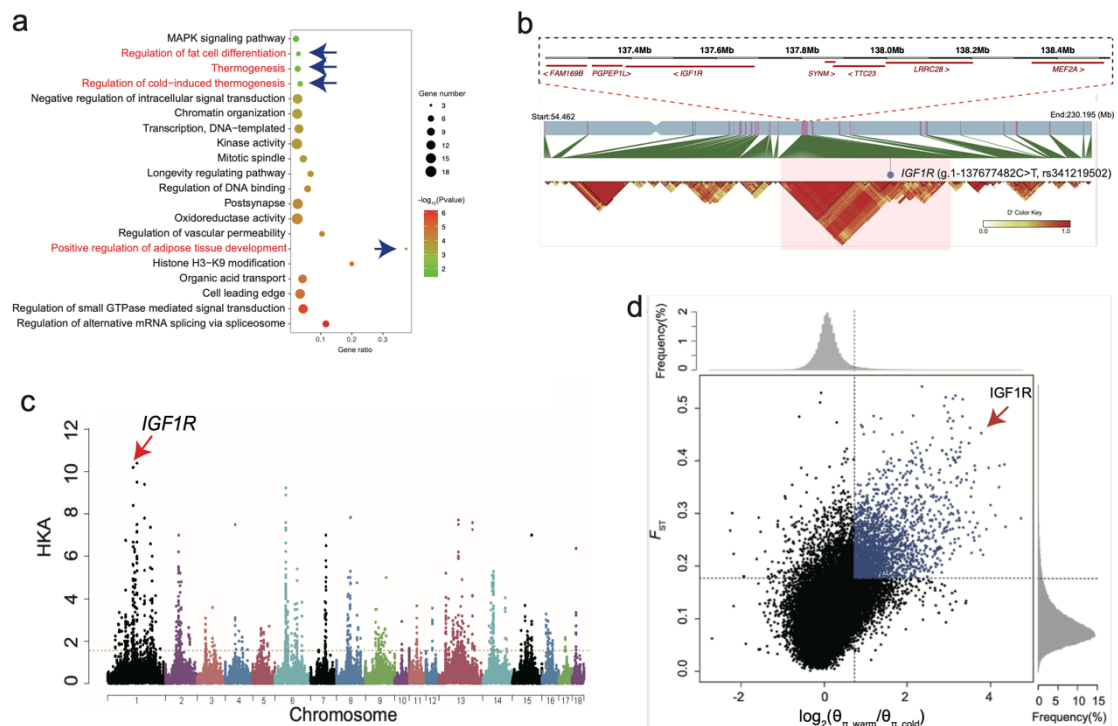


**Figure 3.** (a) The EHH bifurcation diagram for haplotype density and breakdown around the site rs341219502. Ancestral haplotypes are blue and derived ones are red. The line thickness is positively correlated to the density of haplotypes. (b) The EHH "hat" diagram for ancestral and derived haplotypes around *IGF1R* allele rs341219502. (c) The allele frequency distribution for rs341219502 in multiple populations. (d) The EHH bifurcation diagram for haplotype density and breakdown around the site rs327139795. Ancestral haplotypes are blue and derived ones are red. The line thickness is positively correlated to the density of haplotypes. (e) The EHH "hat" diagram for ancestral and derived haplotypes around *BRD4* allele rs327139795. (f) The allele frequency distribution for rs327139795 in multiple populations.

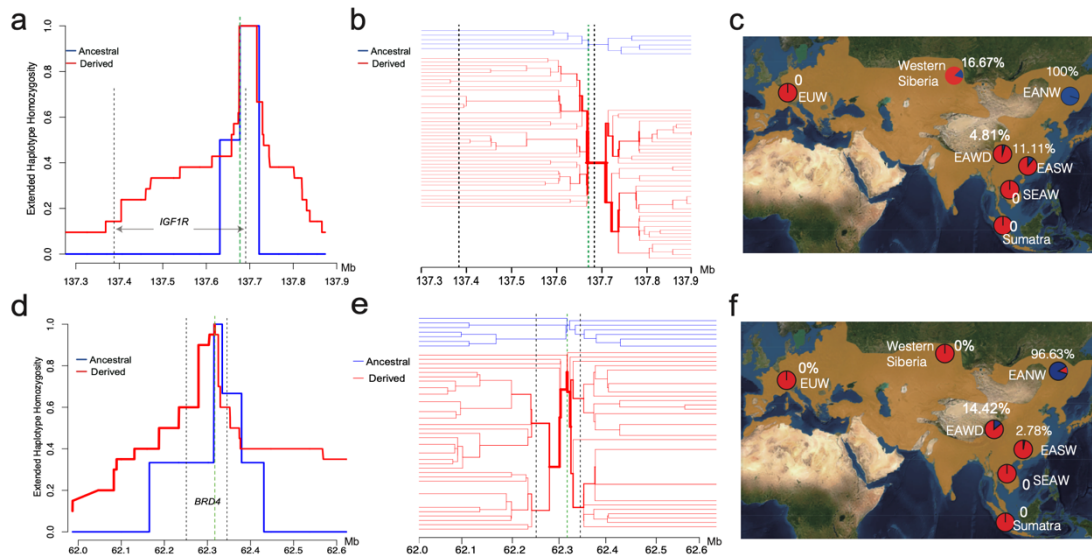


**Figure 4.** The regulatory enhancer mapping and mutational effect of rs341219502.

(a) The RNA-seq expression of *IGF1R* in tissues of fat and diencephalon for the Min pig. (b) The H3K27ac intensity around the gene *IGF1R*. (c) The H3K27ac intensity around the rs341219502 in the *IGF1R* intron. (d) The predicted TF binding sites gained for rs341219502 (C>T) at *IGF1R* intron. (e) The RNA-seq expression profile of TFs in tissues of fat and diencephalon from the Min pig. Note: CPM, or Counts Per Million, is a gene expression normalization to make the expression levels comparable across different samples by accounting for sequencing depth and library size. (f) The expression of *BRD4* in fat and thalamus tissue of Min pig. (g) The H3K27ac intensity around the *BRD4* gene. (h) The H3K27ac intensity around the rs327139795 in *BRD4* exon. (i) The TF binding nearby the rs327139795. (j) The amino acid change of the rs327139795 in exon 6 of *BRD4*. (k) The absence of phosphorylation site in mutant type of rs327139795 in exon 6 of *BRD4*.

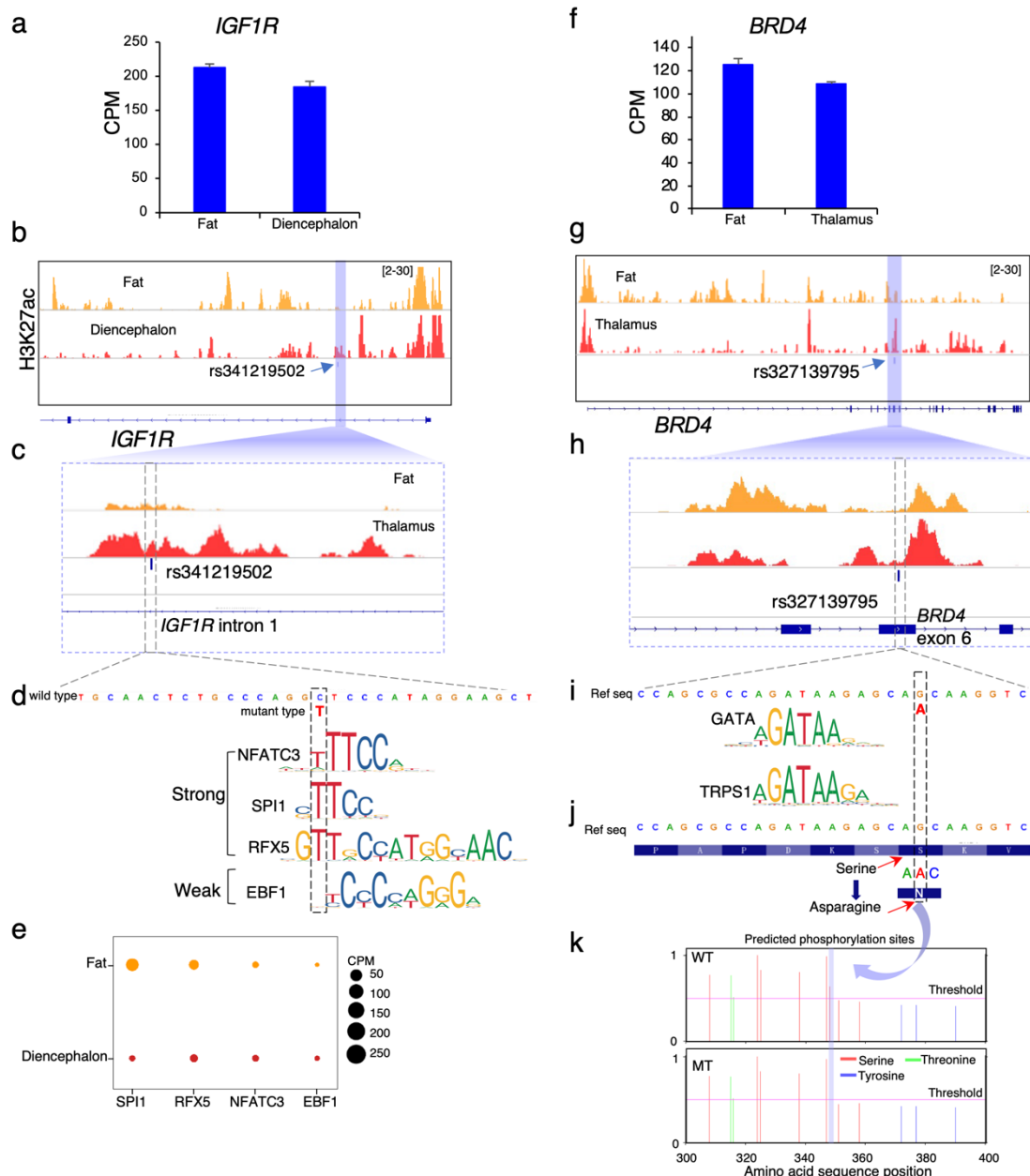
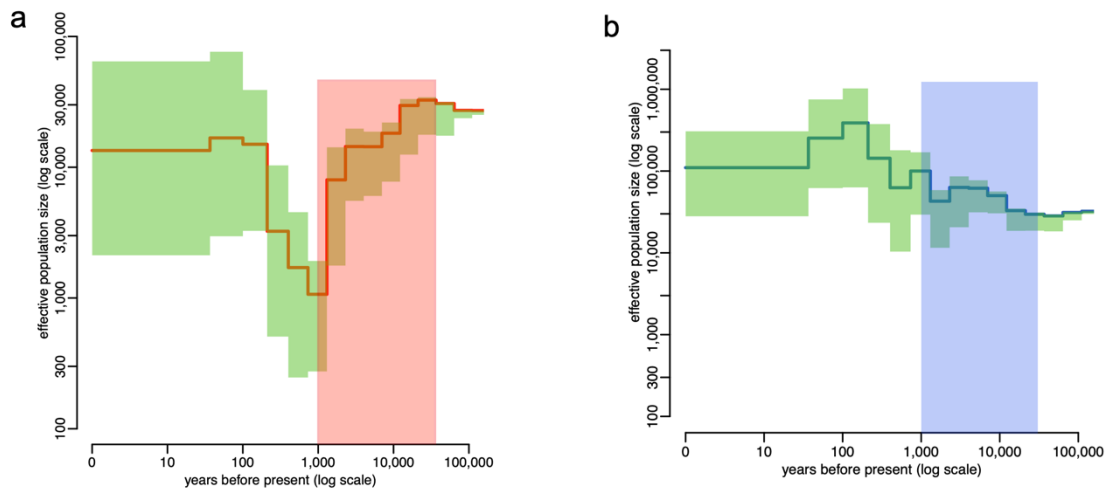
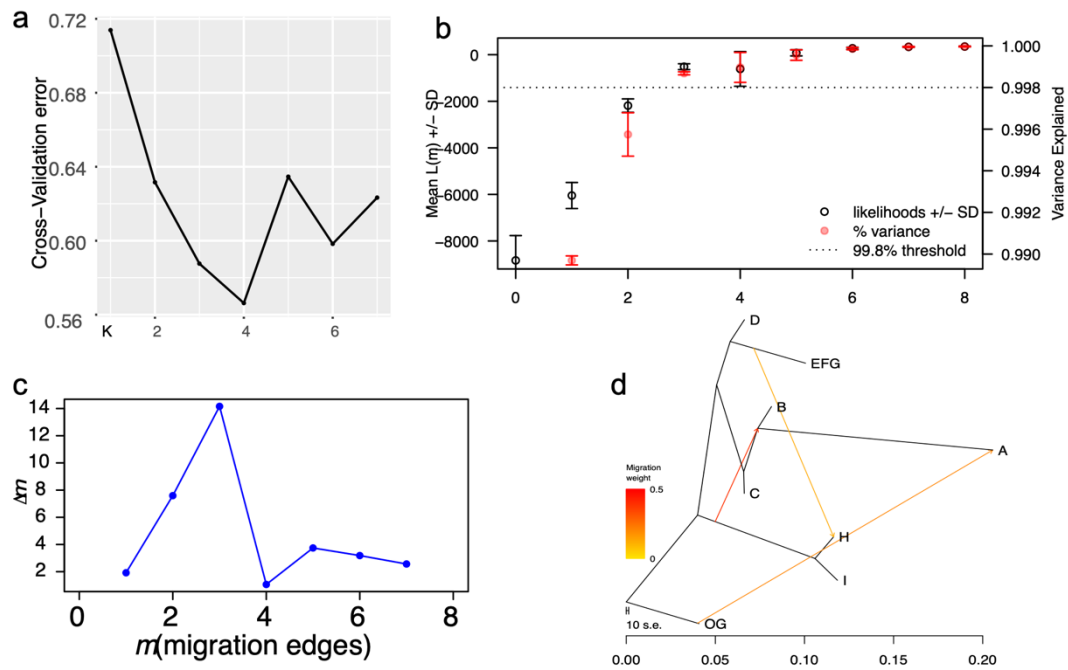


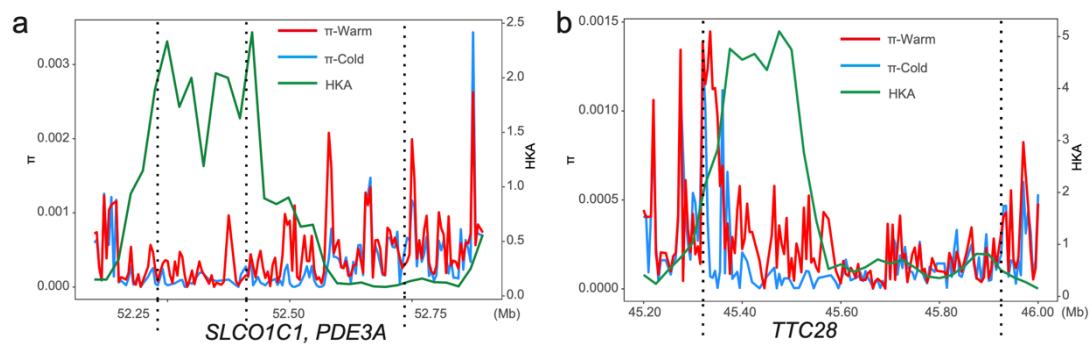
**Figure 5.** The historical demography of warm-region (a) and cold-region wild boar populations (b) inferred with the approximate Bayesian computation (ABC) based method (30). The dotted lines indicate the 5% and 95% quantiles of the posterior distribution. The red and blue frames show the time range from 50,000 to 1,000 years ago. This period also exhibits the lowest prediction error probabilities (<20%, Supplementary Figure 6). The generation time and mutation rate for simulation were based on a previous study (28).



**Supplementary Figure 1.** Gene flow analyses among major populations (a) The cross-validation errors of the ADMIXTURE tool for inferring population ancestry and admixture. (b) The optimal number of migration events (m) for TreeMix based on the inference of OptM estimation. Over 99.8% of the variance was explained when m=3. (c) The  $\delta m$  estimation supported the migration events of 3. (d) The direction of gene flow revealed by TreeMix, based on autosomal SNPs. The gene flow from eastern to western Siberia was detected (EFG  $\rightarrow$  H). Three arrows show the directions from donor populations to recipient populations. Note: all the population codes are the same as in Figure 1a.



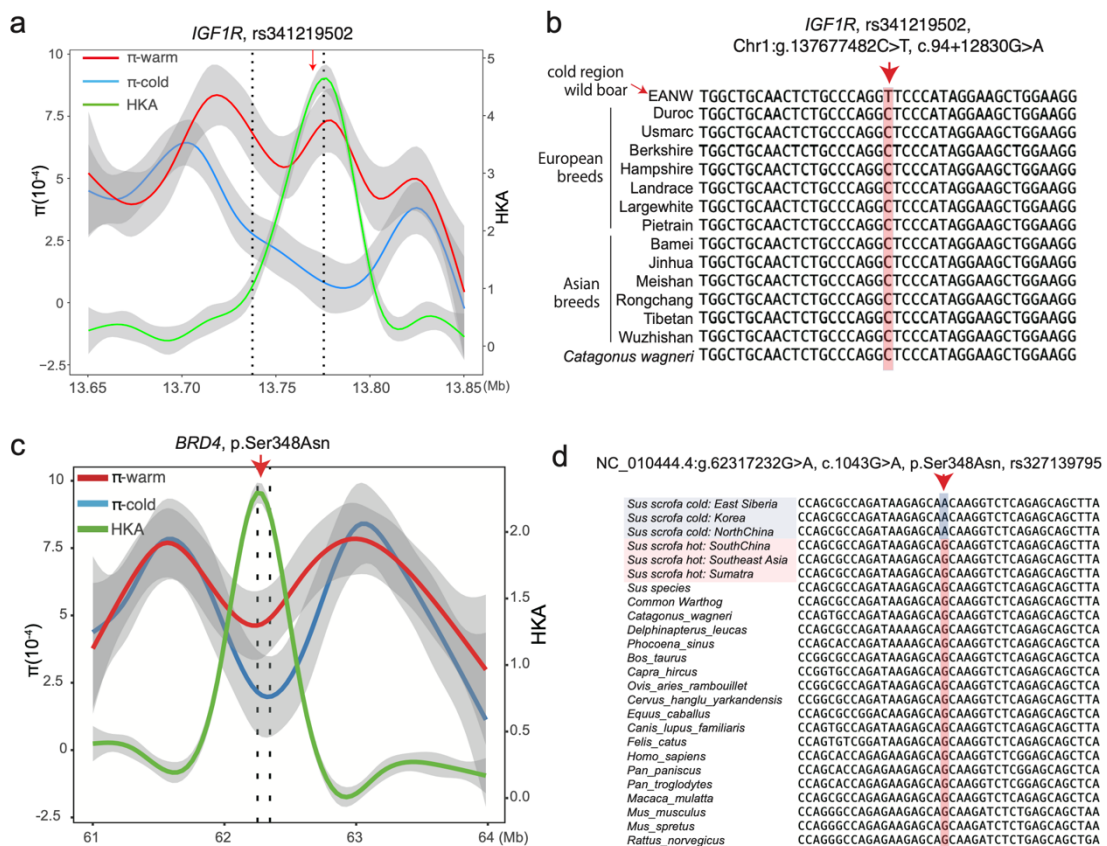
**Supplementary Figure 2.** The warm-cold nucleotide diversity ( $\pi$ ) comparison and HKA test ( $p < 0.01$ ) for the neighboring genes *SLCO1C1* and *PDE3A* (a) and *TTC28* (b). Dotted lines indicate gene boundaries.



**Supplementary Figure 3.** (a) The local signals of *IGF1R* selective sweep based on evidence of nucleotide diversity ( $\pi$ ) for cold- and warm-region populations (left axis) and the polarized HKA test (right axis). The red arrow indicates the site of rs341219502. (b) The population and evolutionary conservation for the ancestral state of rs341219502 ("C") based on the whole-genome alignment. The first sequence represents the mutant sequence of cold-region wild boars. The next 13



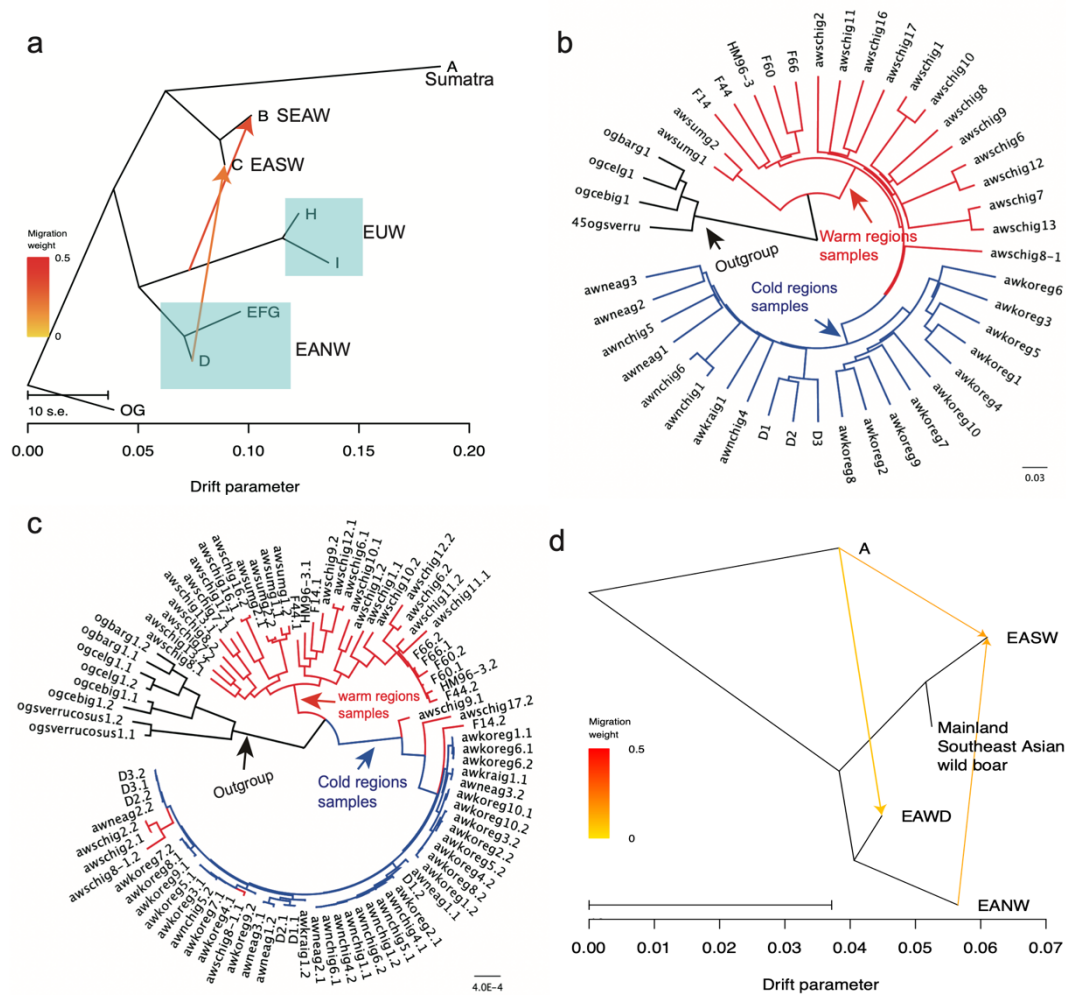
954 sequences are retrieved from genomes of pig breeds in Ensembl (v105) and the last  
 955 sequence shows *Catagonus wagneri* genome (Ensembl v105). (c) The local signals  
 956 of *BRD4* based on evidence of nucleotide diversity ( $\pi$ ) for cold- and warm-region  
 957 populations (left axis) and the polarized HKA test (right axis). The red arrow indicates  
 958 the site of rs327139795. (b) The population and evolutionary conservation for the  
 959 ancestral state of rs327139795 based on the whole-genome alignment.



960  
 961 **Supplementary Figure 4.** The derived allele frequency distribution and the gene  
 962 flow direction. (a) The localized gene flow around variant rs341219502 (600 Kb)  
 963 revealed by TreeMix. Three arrows show the directions from donor populations to  
 964 recipient populations. All population codes are the same as in Figure 1a. (b) The  
 965 background topology of chromosome 1 with a highlight on the two clades of North-  
 966 region (cold) and South-region (warm) populations, represented by blue and red  
 967 branches, respectively. (c) The local haplotype tree of 600 Kb around the

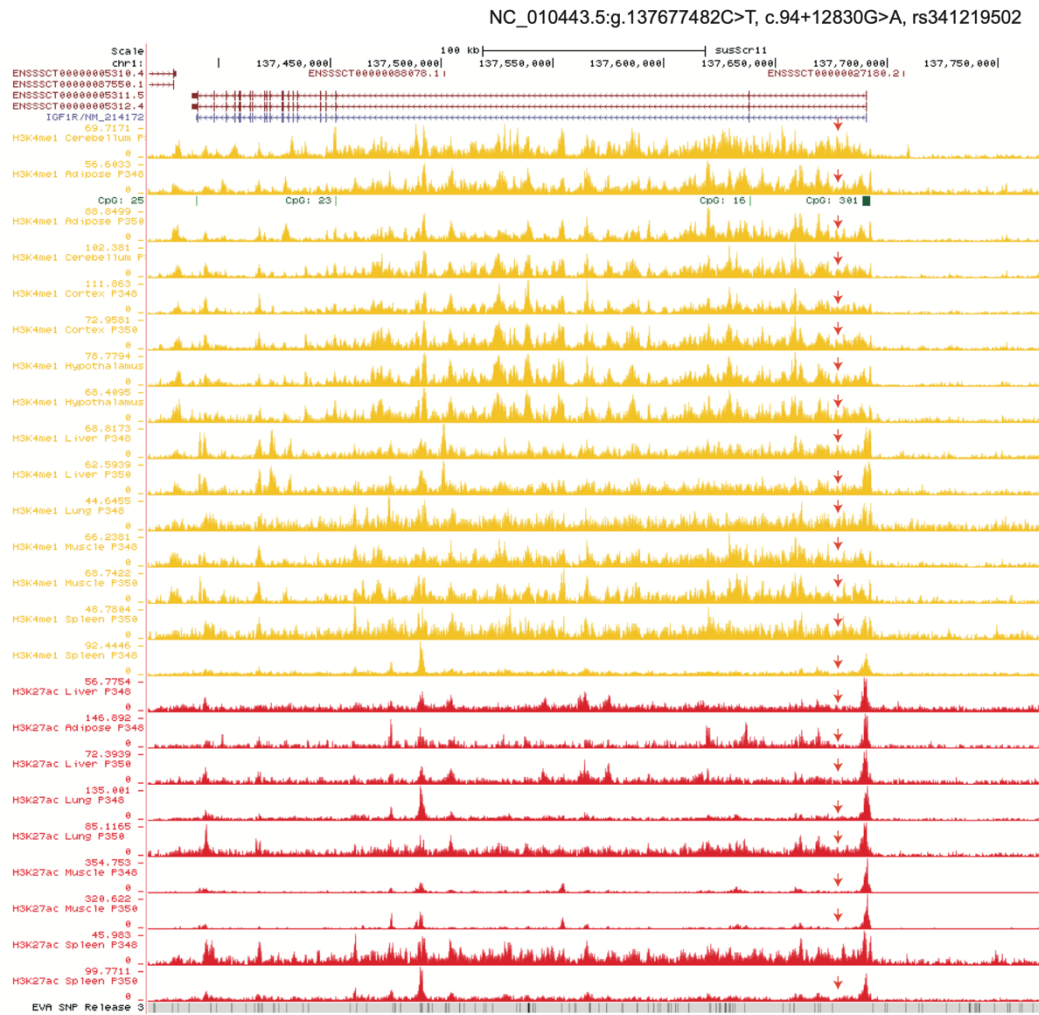


rs341219502 inferred with the Maximum likelihood method of FastTree v2.1. The red haplotypes from the warm-region population were nested into the clade of the cold-region population. The “1” and “2” represent the two haplotypes for each sample. Note: The black asterisks indicate major clade branching with 100% support values. The triangles represent wild boar samples from temperate or tropical regions that are nested within the clade of the cold region. The abbreviations of regions are: EUW, European wild boar; EAWD, East Asian western domestic pigs (Tibetan breed); SEAW, southeastern Asian wild boar; EASW, East Asian southern wild boar; EANW, East Asian northern wild boar (including populations from northern China, Korea, eastern Siberia, and northeastern China). (d) The localized TreeMix migration events (m=3) for the region from 61.5Mb to 63Mb around the 811 selected variant rs327139795 of *BRD4*. The directions of gene flow are shown with arrows.

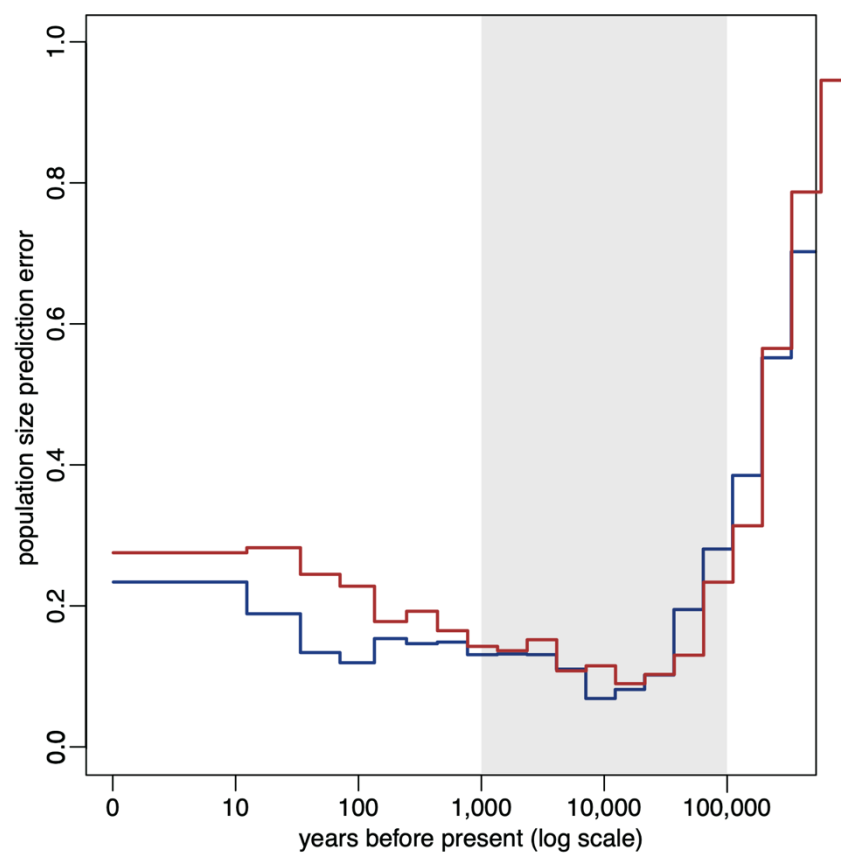


980

**Supplementary Figure 5.** The mapping signals based on H3K4me1 and H3K27ac  
ChIP-seq data retrieved from UCSC Genome Browser  
([http://genome.ucsc.edu/s/zhypan/susScr11\\_15\\_state\\_14\\_tissues\\_new](http://genome.ucsc.edu/s/zhypan/susScr11_15_state_14_tissues_new)). The red  
arrow shows the coordinate to the intronic variant rs341219502 of *IGF1R*.



**Supplementary Figure 6.** The predicted errors for different time stages. The time  
range from 50,000 to 1,000 years ago has the lowest errors (<20%, scaled) under  
the tolerance rate of 0.001. The red and blue lines show the warm- and cold-region  
populations, respectively.



990